[20] Moyer, C. B. and Rindal, R. A., "Finite Difference Solution for the In-Depth Response of Charring Materials Considering Surface Chemical and Energy Balances," Final Rept. 66-7, Pt. II, March 1967, Vidya Div., Itek Corp., Palo Alto, Calif.

[21] Mathieu, R. D., "Mechanical Spallation of Charring Ablators in Hyperthermal Environments," *AIAA Journal*, Vol. 2, No. 9, Sept. 1964, pp. 1621–1627.

[22] Bishop, W. M. and DiCristina, V., "A Prediction Technique for Ablative Material Performance Under High Shear Re-Entry Conditions," *AIAA Journal*, Vol. 6, No. 1, Jan. 1968, pp. 59–63.

[23] Kratsch, K. M. et al., "Graphite Ablation in High-Pressure Environments," AIAA Paper 68-1153, Williamsburg, Va., 1968.

[24] McVey, D. F., Auerbach, I., and McBride, D. D., "Some Observations on the Influence of Graphite Microstructure on Ablation Performance," AIAA Paper 70-155, New York, 1970.

[25] Schneider, P. J., Dolton, T. A., and Reed, G. W., "Mechanical Erosion of Charring Ablators in Ground-Test Reentry Environments," *AIAA Journal*, Vol. 6, No. 1, Jan. 1968, pp. 64–72.

APRIL 1971 J. SPACECRAFT VOL. 8, NO. 4

Measurements of the Dynamical Behavior of Projectiles over Long Flight Paths

WILLIAM H. MERMAGEN*
Ballistic Research Laboratories, Aberdeen Proving Ground, Md.

The yawing and rolling behavior of projectiles is studied using a pair of onboard solar aspect sensors. The instrumentation and data handling procedures used to extract motion information from the data are discussed. Several interesting flights of fin- and spin-stabilized shells are described in detail. Large-amplitude yawing motion and roll reversal with the possibility of resonance have been observed. The pitch frequencies are well determined, and the derived modal amplitudes and phases seem reasonable. Applications and limitations of the technique are discussed.

Nomenclature

C_{M_α} = static moment coefficient
c_0, c_2 = cubic static moment coefficients
I_x, I_y = axial, transverse moments of inertia
K_j = amplitude of the j − mode (j = 1,2)
K_s = amplitude of the projection of the unit solar vector onto the Y-Z plane of the fixed plane coordinate system
k_t = transverse radius of gyration
l = reference length (body diameter)
M_2 = a combination of the linear and nonlinear parts of the cubic static moment
m_j = direction cosines of the unit missile vector (j = 1,2,3)
P = gyroscopic spin
S = reference area ($\pi l^2/4$)
s_j = direction cosines of the unit solar vector (j = 1,2,3)
s = distance along the trajectory (arc length)
t = time
$\mathbf{u}_s$ = unit vector in the direction of the sun
$\mathbf{u}_m$ = unit vector along the missile axis
V = velocity
x = interval between successive sun-sensor pulses
y = interval between alternate sun-sensor pulses
α_t = total angle of attack
β = half-angle between solar sensors on the circumference of the missile
γ = cos α_t
γ_j = angle of inclination between the field of view of the jth sensor and the missile axis (j = 1,2)
ϕ = roll angle
ϕ_j = phase angle of the j modal arm (j = 1,2)
ϕ_s = phase angle of the solar modal arm
λ_j = damping rate of the j modal amplitude (j = 1,2)
ρ = density of air
σ = solar aspect angle (between missile axis and solar vector)
ξ, ξ_g = complex yaw, and complex yaw of repose
ξ_s = complex solar orientation

Superscripts

$(\dot{}), (\ )'$ = $d(\ )/dt$ and $d(\ )/ds$, respectively

Subscripts

0 = initial conditions or zero order
r = reduction or average value

Presented as Paper 70-538 at the AIAA Atmospheric Flight Mechanics Conference, Tullhama, Tenn., May 13–15, 1970; submitted May 28, 1970; revision received December 10, 1970.

* Chief, Physical Measurement Section, Exterior Ballistics Laboratory. Member AIAA.

Introduction

THE pitching, yawing, and rolling motion of projectiles is usually measured in wind tunnels and free-flight ranges using shadowgraph techniques. Until recently no direct measurements of projectile motion over long trajectories have been possible because of the limitations of ground-based instruments. Advances in the art of high-g telemetry have permitted the instrumentation of projectiles with active electronic payloads.[1–5] These onboard instruments are designed to survive accelerations up to 100,000 g during gun-launch. Solar aspect sensors[6] and accelerometers have been developed to observe the motion of the projectile. A yawsonde built by the British and used by the Naval Weapons Center (NWC) China Lake, in a small number of flights.[7] A Harry Diamond Laboratories modification of this sonde has also been used by NWC.

The Ballistic Research Laboratories have developed a yawsonde of different design and have successfully instrumented a number of projectiles to obtain data on yawing and rolling motion. This paper describes the onboard solar aspect sensing instrument, calibration and analysis techniques, data handling and reduction processes (manual and automated), accuracy limitations, results of recent firings, and limitations of and usefulness of this technique.

Measuring System

The solar aspect angle σ (Fig. 1) can be measured by a simple geometric arrangement of sensing cells and slits. Two silicon solar cells are mounted in fixtures which define almost planar fields of view (Fig. 2). Each field of view is established by a slit, serrated along its length to absorb internal light reflections, with reflective surfaces at each end of the slit to permit wide viewing in the plane. The angle 2β between the two fixtures in a plane perpendicular to the projectile axis (Fig. 3b) is set to a predetermined value. As the projectile rolls, the sun is intercepted by each fixture in turn at a time when the solar vector lies in the plane of the field of view of that fixture. The time interval y between successive intercepts of the sun by the same cell fixture is the period of the rolling motion. The time interval x between successive intercepts by two-cell fixtures is related to σ. These statements are exactly true provided the projectile does not change its angle of attack during a single revolution and the roll rate is constant.

The sensor pulses are amplified, changed in polarity, and fed to a voltage-controlled oscillator (VCO) operating at one of the IRIG (Inter Range Instrumentation Group) frequencies. The VCO in turn modulates a radio-frequency oscillator operating in the VHF band from 215 to 260 MHz. The result is an FM/FM telemetry system which provides noise-free data transmission. Pulse risetimes are limited by the center frequency of the VCO which was selected at 70 kHz, providing a pulse risetime capability of about 25 μ sec. Faster rising pulses are reduced in amplitude but still transmitted. The transmitter develops 50 mw into a 50-ohm load. The antenna consists of an asymmetrical dipole formed by insulating the nose of the projectile from the remainder of the vehicle. The insulator is usually a threaded fiberglass junction. During assembly, the nose, the fiberglass section, and the body of the shell are torqued together to prestress the joint at ~10,000 psi to prevent failure of the junction during high-acceleration launch. The impedance of the transmitter is matched to the antenna using a capacitive network. The radiated power output is in the order of tens of milliwatts.

The ground-receiving station consists of high-gain antennas, FM receivers, magnetic tape recorders, and oscillograph recorders. The received radio signal is demodulated and the video information (VCO frequency) and a range-timing signal are recorded on magnetic tape. Playback of the tape can be done at leisure. The recorded VCO signal must be further discriminated to provide the sun-sensor pulse train for data reduction. The pulses can be graphically displayed on an oscillograph or on an oscilloscope equipped with moving film camera.

Calibration

The telemetry link does not require calibration, since it merely transmits the pulses without regard for amplitude accuracy. The electronics on board the projectile and on the ground do not introduce phase errors into the relationships between the pulses. A calibration on the geometry of the solar sensing assembly is needed. Two types of calibration are possible: 1) geometric calibration by measuring the angles of installation of the solar cell fixtures and deriving a formula relating σ to the pulse spacing through the installation angles, and 2) physical calibration using a light source to simulate the sun. Calibration data relating σ to the roll intercepts of the light source are taken.

The geometric calibration is easier to use. Figure 2a shows the pulse train and the measurement variables x and y. The ratio x/y is related to σ by the following relation:

$$\tan\sigma = \tan\gamma_1(1 + A^2 + 2A\cos\alpha)^{1/2}/\sin\alpha \qquad (1)$$

where $\alpha = 2(\pi x/y - \beta)$, and $A = \tan\gamma_2/\tan\gamma_1$, and the angles γ_j (j = 1 or 2) and β are illustrated in Fig. 3b. If the roll rate varies by as little as 1%, errors of several degrees will be introduced into the data. One can correct for such variation if it is known, and it can be obtained from the data. The angle 2β is known to an accuracy of ~1 arc min, and γ_1 and γ_2 are determined by photographic techniques to within 15 arc min. The cumulative error due to these inaccuracies also depends on the ratio x/y. For γ_1 and γ_2 in the neighborhood of 45° and β = 75°, the maximum error is less than 0.5° in σ.

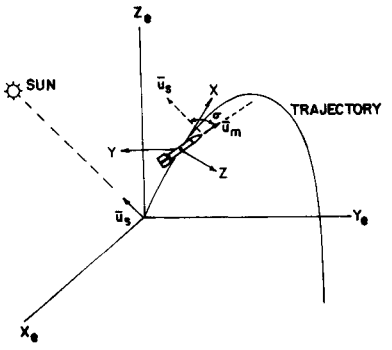

Fig. 1 Coordinate system geometry.

In a physical calibration system, a carbon arc light source and a collimating lens system provide parallel light, which is mechanically chopped and allowed to fall incident on the projectile. The shell is mounted in a fixture which permits rotation of the shell about its longitudinal axis and an orthogonal axis, so that rolling and pitching motion can be simulated. The onboard electronics are turned on, and a ground station is set up to receive the pulse data and display them on an oscilloscope. First the shell is inclined with respect to the light source to simulate a given σ, then it is rotated about its longitudinal axis until each sensor in turn detects the chopped light. The dynamic variable x/y is simply the change in roll angle per revolution, $\Delta\phi/2\pi$. A table of σ vs x/y is obtained by continuing this procedure through various values of σ. The present calibrator can resolve 5 arc min in roll and about the same in σ. The cumulative error is ~0.2°.

Instrumented projectiles were calibrated by both methods, and the results agreed within 0.5° over the entire span of σ.

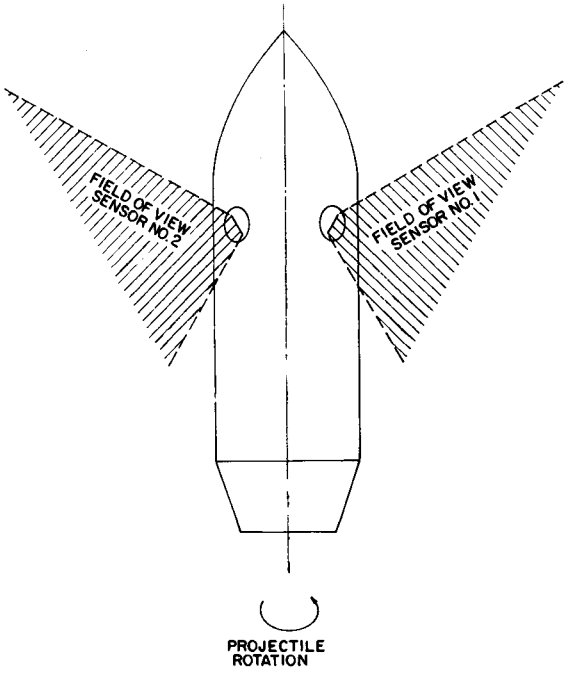

Fig. 2 Orientation of solar sensor fields of view.

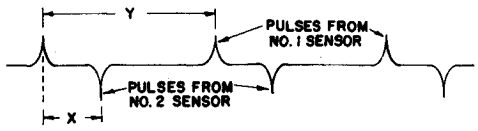

Fig. 3a Pulse train from mixed and inverted solar sensor pulses.

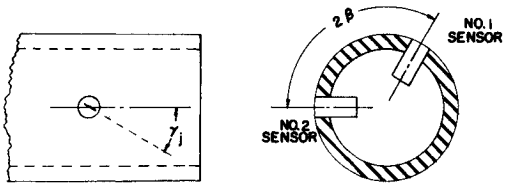

Fig. 3b Sensor inclination and orientation angles needed for geometric calibration.

It should be noted that the range of σ which can be measured depends on the γ_j; if they are large, then only small values of σ can be observed, but the accuracy of observation is increased. Conversely, if the γ_j are small, then a wide range of σ can be observed, but accuracy suffers. Since the fixtures can be installed to any desired inclination, a very flexible system results.

Data Handling and Reduction

The primary data from a test flight consist of pulses of alternating polarity. The phase relationship between pulses contains the σ information. The pulse frequency equals the roll rate; since most spinning projectiles have roll rates between 10 and 400 rps, and times of flight between 20 and 300 sec, the number of pulses per flight can vary from 200 to 120,000.

For manual data reduction, x/y is obtained for each pulse interval as a function of time by reading the graphic display with an optical-mechanical reader having a resolution of one part in 10^4. The roll rate is obtained directly and examined to determine the change in roll rate per revolution. A smoothed calibration is applied to the data giving $\sigma(t)$. With the data in this form, the trajectory vector and solar vector can be included in the reduction program, and the data can be fitted to an exact relation between σ, modal amplitudes and frequencies as described later. The accuracy of the data reduction must be such that the location of a given pulse is known with respect to a subsequent pulse to within 0.3% to keep the error in σ below 0.5°.

The automatic reduction technique is designed for use with a hybrid computer. The data tapes are played back through a discriminator into the analog section of the hybrid, which can be programmed to handle the data in a variety of ways. Consistent results have been obtained by two methods, one using integrators, and the other using counters. In the former, the pulses are used to start and stop two integrators, which provide voltages that vary linearly with time. One pulse starts an integrator, the next pulse samples the voltage, and the third pulse stops the integrator and samples its voltage. The third pulse also starts the second integrator, which runs while the first integrator recycles. The two integrators provide voltages proportional to x and y. In the counter technique, pulses start and stop internal counters in the analog section of the hybrid, and the ratios of counter periods are the required x/y data. The minimum time resolution is 1 μsec, allowing the hybrid to handle spin rates up to about 500 rps.

With either method, the output of the analog section is fed into the digital part of the hybrid. Time is derived from an internal clock in the analog section. In the digital part of the computer the calibration is applied to the x/y data producing $\sigma(t)$. The time is taken at the first pulse of a 3-pulse ensemble. The output of the digital section is formatted on digital tape for fitting with trajectory and σ data.

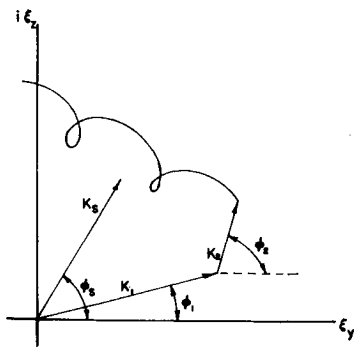

Fig. 4 Geometric description of modal amplitudes in the missile-fixed plane coordinate system.

Analysis

The σ data do not directly give the motion of the projectile; by itself, σ simply defines the semiapex angle of a conical surface on which the missile axis lies. One also must know the local tangent to the trajectory (usually available from radar tracking of the shell) and the location of the sun to determine the motion of the projectile, which, for this analysis, is assumed to be epicyclic.

Several approaches to handling σ data have been suggested. One can begin with the equations of motion of the shell, assume a certain type of motion, and vary the aerodynamic coefficients until the σ data and the solution to the equations of motion agree, as NWC has done on an analog computer.[7] Another approach is to fit the equations of motion to the data directly.[8] A third method is to assume the form of the solution to the equations of motion and fit the data to the solution using several cycles of the motion at a time, as done by Eikenberry and Nicolaides in a computer program called WOBBLE.[9] The method currently in use at the BRL is a modified version of the WOBBLE program.

Geometric Relationships

It is convenient to define a cartesian coordinate system whose origin is fixed at the center of mass (c.m.) of the projectile and moves with the projectile along its trajectory. The X axis of the system is tangent to the trajectory and positive in the direction of increasing arc length; the Y axis is perpendicular to the plane of the trajectory. This "trajectory" or "range" coordinate system is shown in Fig. 1 relative to an Earth-fixed system. Let $\mathbf{u}_m$ be a unit vector along the axis of the projectile and $\mathbf{u}_s$ be a unit solar vector directed from the c.m. to the sun; $\mathbf{u}_s$ is constant if the sun does not change position during the flight of the projectile and if the apogee altitude is small compared to the distance to the sun. Then

$$\cos\sigma = \mathbf{u}_s \cdot \mathbf{u}_m \tag{2}$$

where the vectors are defined in the range coordinate system as

$$\mathbf{u}_m = (m_1, m_2, m_3) \quad \text{and} \quad \mathbf{u}_s = (s_1, s_2, s_3) \tag{3}$$

The solution to the equations of motion[10] of a symmetrical shell for small amplitude motion is expressed by

$$\xi = K_1 e^{i\phi_1} + K_2 e^{i\phi_2} + \xi_g \tag{4}$$

where $|\xi| = \sin\alpha_t$ and epicyclic behavior is assumed. Since the projectiles under discussion herein are spinning slowly and only short portions of the trajectory are considered, the ξ_g term due to gravity can be dropped. If the motion were

tricyclic, a K_3 mode with phase ϕ_3 would be needed in addition to the K_1 and K_2 modes.

The K_1 and K_2 modal arms lie in the Y-Z plane of a missile-fixed plane coordinate system where the X axis is the missile axis. This representation is shown in Fig. 4. The vectors, Eq. (3), are expressed in a range coordinate system. The transformation from range coordinate system to missile-fixed plane coordinate system is accomplished by

$$m_1 = [1 - (\xi_y^2 + \xi_z^2)]^{1/2} \qquad s_1 = [1 - (\xi_{sy}^2 + \xi_{sz}^2)]^{1/2} \quad (5)$$

$$m_2 = \{\xi_y^2/(1 - \xi_y^2)[1 - (\xi_y^2 + \xi_z^2)]\}^{1/2} \quad (6)$$

$$s_2 = \{\xi_{sy}^2/(1 - \xi_{sy}^2)[1 - (\xi_{sy}^2 + \xi_{sz}^2)]\}^{1/2} \quad (7)$$

$$m_3 = [\xi_z^2/(1 - \xi_y^2)]^{1/2} \qquad s_3 = [\xi_{sz}^2/(1 - \xi_{sy}^2)]^{1/2} \quad (8)$$

where

$$\xi = \xi_y + i\xi_z, \qquad \xi_s = \xi_{ys} + i\xi_{zs} = K_s e^{i\phi_s} \quad (9)$$

Using Eq. (2) with the transformation relations (5–9), an exact but complicated relation between σ, $\mathbf{u}_s$, solar vector, and the modal arms can be derived. This complicated relation can be simplified, ignoring terms greater than third order in K_j and the following expression results

$$\cos\sigma = \{1 - \tfrac{1}{2}K_s^2 - \tfrac{1}{2}[K_1^2 + K_2^2 + 2K_1K_2\cos(\phi_1 - \phi_2)]\} + K_sK_1\cos(\phi_1 - \phi_s) + K_sK_2\cos(\phi_2 - \phi_s) \quad (10)$$

The phase angles are stated in terms of initial phase angles and frequencies

$$\phi_j = \phi_{j0} + \phi_j' s \quad (11)$$

For small angles, then, we can fit the data by Eqs. (10) and (11) with six parameters to the fit: K_1, K_2, ϕ_{10}, ϕ_{20}, ϕ_1', and ϕ_2'. The frequencies can be related if the spin is known. For large angles,[10]

$$\phi_{1r}' + \phi_{2r}' - \tfrac{1}{2}(K_1^2\phi_{1r}' + K_2^2\phi_{2r}') = P + M_2[(K_1^2 - K_2^2)/(\phi_{1r}' - \phi_{2r}')] \quad (12)$$

where ϕ_{jr}' are the data reduction values of the frequencies in the missile-fixed plane coordinate system, P is the gyroscopic spin, and M_2 is a combination of the linear and nonlinear parts of the cubic static moment.

$$M_2 = (c_2 - \tfrac{1}{2}c_0)\rho Sl/2mk_t^2 \quad (13)$$

M_2 vanishes if the static moment varies directly with $\tan\alpha_t$. Such behavior, however, has not been noticed in shells, and M_2 must be taken into consideration if geometrical angles are large.

Equations (12) and (13) can be used to reduce the number of parameters of the fit from six to five. If the amplitude of motion is small, Eq. (12) becomes simply $P = \phi_1' + \phi_2'$. Conversely, if the amplitude of motion is large, and the parameters of fit are kept at six, allowing both frequencies to be free in the fitting process, it might be possible to extract M_2 from the fit of the data using Eqs. (12) and (13). The gyroscopic spin and the arc length are measured, and the density is taken from standard atmospheric tables.

The fitting procedure uses the method of differential corrections with least squares: initial values are estimated, differential corrections are taken, a least squares fitting is done to obtain new values, the new values are substituted into the fitting process, and the procedure continues (iteratively) until either convergence or diverence occurs. Convergence to a best fit in the least squares sense will occur if the original estimates are resonably close to the converged values. Thus, with a five- or six-parameter family to be fitted, a large field of original estimates must be considered. A variety of initial estimates should be considered in the reduction procedure,

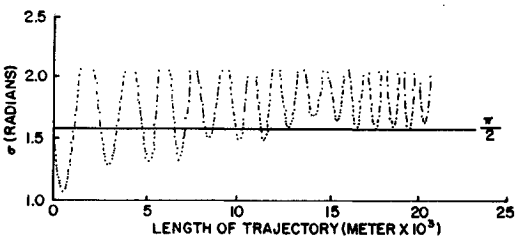

Fig. 5 Raw data from HARP 5-in. projectile postsummital yaw.

since the process may converge to local minima. A judicious selection of fitted results based on standard error and the progress of fits of subsequent data points must be made.

Aerodynamics

The result of data reduction is a set of values of the modal amplitudes, phase angles, and frequencies as a function of arc length along the trajectory. The damping exponents can be determined from the change in modal amplitude with arc length. An average static moment coefficient $|C_{M\alpha}|_r$ can be computed directly from the reduced frequencies.

The drag coefficient can in theory be computed from a fit of the radar-resolved trajectory. In practice, the trajectory data are usually not smooth enough to permit accurate determination of drag. The Magnus and damping moment coefficients can be obtained from the data if an independent measurement of the lift coefficient is available. The techniques for extracting aerodynamic coefficients from the data are well outlined by Murphy.[10]

Accuracy

The over-all accuracy of the solar aspect sensing system is $\pm 0.5°$ in σ. The data handling technique introduces less than $\pm 0.5°$ error. Thus, the cumulative error is within $\pm 1.0°$. In the differential-corrections, least-squares data fitting process, only those converged values are selected with standard error less than experimental error.

There is no test or guarantee that the results of the fitting process are unique. A wide variety of initial estimates on the fitting parameters will give convergence for a single cycle of variation of the data. In the 5- or 6-parameter space of the fit, it seems that a large variety of local minima exist at which convergence will occur. The absolute minimum, if one exists, can only be determined by trial and error. If many cycles of data are used in the fit, then the number of convergent solutions should be smaller. Fortunately, many of the minima at which convergence takes place yield values of the parameters which give standard errors several orders of magnitude greater than the experimental error and can be readily discarded. A selection among the remaining fitted values can be based on the lowest value of standard error and on the subsequent fitted values of the parameters. The results can be compared with values of the aerodynamic coefficients obtained from range measurements to give added confidence that the results are reasonable.

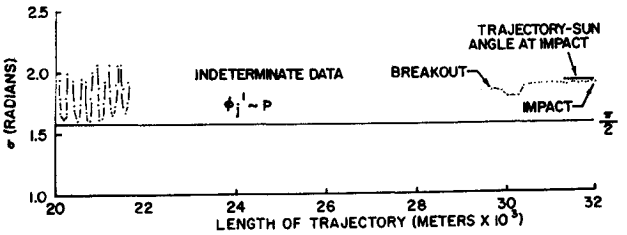

Fig. 6 Raw data from HARP 5-in. projectile (continuation of Fig. 5 data).

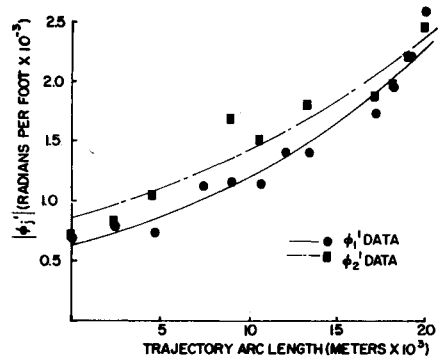

Fig. 7 Frequencies of the modal arms as a function of trajectory arc length.

Results

A number of 5- and 7-in.-diam HARP projectiles have been instrumented with solar aspect sensors and data on high-angle-of-fire trajectories have been obtained. In addition, the Harry Diamond Laboratories yawsonde has been used on board some M329Al and M329AlEl mortar rounds with success.[11] Large-amplitude yawing motion during the descent of a 5-in. projectile from apogee has been observed and provided the test case for the development of the analysis and reduction program. Roll reversal was observed on another 5-in. firing.

Large Amplitude Yaw

The HARP 5-in. projectile[12] is an arrow projectile with slightly canted fins. (With uncanted fins are achieved very low altitudes on 3 of 4 flights; 2° or 3° cant on the fins produces a roll rate of ~10 rps and seems to assure a high apogee. It was originally decided to instrument this projectile to determine the cause of poor altitude performance with straight fins. At present we have been unable to duplicate a poor flight with a σ sensing system on board, but some interesting results have been obtained from the canted fin flights.) Figure 5 shows a part of the σ vs arc length (s) data shortly after the summit of a trajectory. The projectile begins its descent with its tail pointing earthward. At some time later it turns over and begins to execute large-amplitude yawing motion. Zero arc length in Fig. 5 refers to the beginning of the large-amplitude motion. The sun-sensor instrument had been preset with $\gamma_1 = \gamma_2 = 30°$, hence the span of measurement is restricted to $\pm 30°$ about the normal to the shell axis. The data clearly show that the amplitude of motion is greater than the measurement span of the sensors in that segments of the data are missing.

Figure 6 shows $\sigma(s)$ during the remainder of descent. Several interesting features of the data can be noted. The frequency of the data increases as the projectile descends into a denser atmosphere and increases in velocity. As the frequency of the yawing motion approaches the roll rate, fewer data points per cycle of motion are available. Finally, when the yawing frequency and roll rate are comparable, the data become indeterminate, because a complete revolution of the shell in roll is needed to establish a measurement of σ. If α_t changes significantly during a single revolution, the measurement becomes meaningless. The projectile breaks out of its large-amplitude motion just before impact. The aspect angle at impact is compared with the angle between the trajectory and the sun at impact. The difference is less than 0.5°, implying that the projectile is not yawing at impact.

The raw data of Figs. 5 and 6 were fitted by Eq. (10) to obtain values of the modal amplitudes, phases, and frequencies. Although a number of initial estimates converged to different values of these parameters, the frequencies ϕ_j' seemed to be well determined and independent of the choice of initial estimates. The constraint imposed by Eq. (12) seems to fix the frequencies. Frequency and roll rate are, of course, the dominant characteristics of the data, and it should not be surprising that they are well determined. The smoothed $|\phi_j'|$ are shown in Fig. 7 as a function of s. Although there is scatter, definite trends can be seen. These fits were taken from the data one cycle at a time. Smoother average frequencies should be expected from a WOBBLE reduction where several cycles are taken at a time.

A check on the magnitude of these frequencies can be made by computing an average C_{M_α} and comparing with range measurements. Figure 8 shows a computed average C_{M_α} vs Mach number. A smooth curve has been drawn through the computed points. The point indicated by the square is taken from a single range measurement of C_{M_α} at Mach 4.4. The curve for the Tl44E2 projectile is included for comparison; this round is similar in shape to the 5-in. projectile and was the basis for the original design of the 5-in. round.

Roll Reversal

An interesting set of data resulted from the firing of another HARP 5-in. projectile under slightly different launch conditions. This projectile was equipped with solar aspect sensors, canted fins, and an in-flight yaw inducer (a small explosive device propelled a brass slug out of the side of the projectile, imparting an overturning moment to the projectile). It was launched at 1540 m/sec at a gun elevation of 40°. Solar aspect sensing data were received immediately as the projectile left the muzzle, and the yaw inducer functioned on time, 5 sec after launch. The most interesting data came from the roll history (Fig. 9).

The characteristics of the solar aspect sensor are such that the direction of spin can be determined unambiguously if the direction of flight is known. In Fig. 9 the data show that the

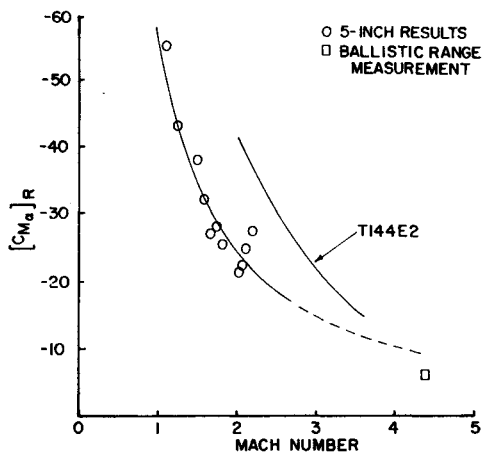

Fig. 8 $C_{M\alpha}$ vs Mach number.

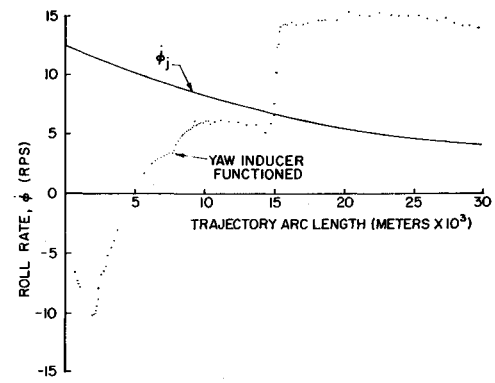

Fig. 9 Roll rate history of 5-in. projectile.

projectile began its flight rolling in a direction opposite to that which the fin cant should produce. The roll rate increased to a maximum of about 10 rps in the negative sense and then reversed. At about 13,000 m down the trajectory, the roll rate approaches steady state when the yaw inducer functions. The roll rate changes and approaches a new steady state value when suddenly, at 15,000 m, the rate jumps to about 15 rps. This rate is maintained throughout the midcourse of the trajectory and gradually decreases to about 5 rps just before impact (not shown in the figure).

Figure 9 also shows a theoretical pitch frequency history. The curve is labeled $\dot{\phi}_j$. The pitch frequency decays gradually from an initial value of 12 rps to 7 rps at the point at which the roll rate shows a sudden increase. The nearly coincidental values of pitch frequency and roll rate just before the sudden increase in roll rate suggest some interaction between pitching and rolling motion.

Discussion and Summary

The large-amplitude motion of an experimental projectile has been observed during the reentry phase of its flight using solar aspect angle (σ) sensors. These data were treated with a quasi-linear analysis and the reduced values of the frequencies seem reasonable. The comparison between a ballistic-range-determined value of static moment (C_{M_α}) and the C_{M_α} derived from the σ data indicates that a quasi-linear approach may be used. The shape of C_{M_α} vs Mach number curve is close to that obtained from range measurements of a similarly shaped projectile. The data reduction procedure gives average values of the aerodynamic parameters since at least a single cycle of the motion must be fitted. If many cycles of the motion produce continuous σ data, a WOBBLE approach can be used in the reduction.

Accurate results can be obtained only if the roll rate is at least an order of magnitude greater than the pitch frequency. This criterion was not met for most of the finned HARP projectiles tested. Most of the tests, therefore, resulted only in roll rate data. Artillery shells, however, spin at much higher rates, and current plans include the instrumentation of a number of 155mm and 175mm shells.

A 5-in. HARP projectile experienced roll reversal, which the interior ballistics of the system may have caused. The projectile is loaded in the gun with bags of powder surrounding the boom of the shell ahead of the fins. This extra powder is needed to assure maximum muzzle velocity. Uneven burning of the powder could produce a torque on the fins in a direction opposed to the aerodynamic torque due to the bevel on the fin surfaces. The sudden jump in roll rate later in the flight may be attributed to coupling between pitching and rolling motion.

Further work in developing aspect sensors which are independent of roll is needed to provide data on slowly rolling finned projectiles. The accuracy of the results obtained from the current aspect sensors can be increased by changing the geometry of the sensor installation at the cost of some loss in solar acceptance angle. Accuracies of 0.1° in yaw are possible for a high-spin-rate shell. For this accuracy, the solar acceptance angle would be reduced to ~30°. Large quantities of raw data are produced by the aspect sensors, and the reduction procedure is tedious even when automated. Data such as presented in this paper, however, have been previously unattainable using conventional range instrumentation. These data furnish useful information over long trajectories and point to problem areas in stability.

References

[1] Mermagen, W. H., Cruickshank, W. J., and Vrataric, F., "VHF and UHF High-G Telemetry for HARP Vehicles," *The Fluid Dynamic Aspects of Ballistics Conference Proceedings No. 10*, Advisory Group for Aerospace Research and Development, 1966, pp. 439–464.

[2] Mermagen, W. H., "Miniature Telemetry Systems for Gun-Launched Instrumentation," *Proceedings of the Fourteenth International ISA Aerospace Instrumentation Symposium*, Instrument Society of America, Vol. 14, 1968, pp. 225–235.

[3] Mermagen, W. H., "Telemetry Experiments Conducted on the HARP Project in British West Indies and Wallops Island, Virginia, During the Period Jan–Mar 1964," MR-1578, July 1964, Ballistic Research Labs., Aberdeen Proving Ground, Md.

[4] Evans, J. W., "Development of Gun Probe Payloads and a 1750 Mc/s Telemetry System," MR-1749, May 1966, Ballistic Research Labs., Aberdeen Proving Ground, Md.

[5] Wilkin, N. D., "TM Research Program—High-g Tests of Components," TM-65-33, July 1965, Harry Diamond Lab., Washington, D. C.

[6] Mermagen, W. H., "HARP 250 Mc/s Telemetry Experiments, Wallops Island, March 1965," MR-1694, Sept. 1965, Ballistic Research Labs., Aberdeen Proving Ground, Md.

[7] Haseltine, W. R., "Yawing Motion of 5.0" MK41 Projectile Studied by Means of Yaw Sondes," TP-4779, Aug. 1969, Naval Weapons Center, China Lake, Calif.

[8] Chapman, G. T. and Kirk, D. B., "A Method for Extracting Aerodynamic Coefficients from Free-Flight Data," *AIAA Journal*, Vol. 8, No. 4, April 1970, pp. 753–758.

[9] Eikenberry, R. S., "Analysis of the Angular Motion of Missiles," SC-CR-70-6051, Feb. 1970, Sandia Labs., Albuquerque, N. Mex.

[10] Murphy, C. H., "Free Flight Motion of Symmetric Missiles," R-1216, July 1963, Ballistic Research Labs., Aberdeen Proving Ground, Md.

[11] MacAllister, L. C. et al., "The Effect of a Subcaliber Cylindrical After-Body on the Behavior of Spin-Stabilized Projectiles," AIAA Paper 70-558, Tullahoma, Tenn., 1970.

[12] Marks, S. T. and Boyer, E. D., "A Second Test of an Upper Atmosphere Gun Probe System," MR-1464, April 1963, Ballistic Research Labs., Aberdeen Proving Ground, Md.